Final manuscript for J. IES, **25**-1, 13-22 (1996)

Realization of NIST 1995 Luminous Flux Scale using Integrating Sphere Method

Y. Ohno
Radiometric Physics Division
National Institute of Standards and Technology
A305, Metrology, Gaithersburg, MD 20899
Phone : (301) 975-2321 Fax : (301) 840-8551

Abstract

A new NIST luminous flux scale has been realized using the integrating sphere method, on which theoretical and experimental studies were previously conducted and reported. The NIST 2 m integrating sphere was modified to add an opening and an additional baffle to apply this method. Flux from an external source (1000 W quartz halogen lamp) is introduced into the sphere through a limiting aperture and the opening. The flux entering the sphere is determined from the measured area of the aperture and the illuminance on the aperture plane measured with the NIST standard photometers that maintain the NIST illuminance scale. The total luminous flux of a group of standard lamps measured inside the sphere is deduced by comparison to the flux from the external source. Corrections are made for the spatial non-uniformity and the incident angle dependence of the sphere response, and the spectral mismatch of the integrating sphere photometer responsivity. The total luminous flux measured with the integrating sphere system is compared to the values obtained with a goniophotometer of PTB, Germany. The values obtained by the two methods agreed to within 0.2 %. The magnitude of the new NIST luminous flux unit is 1.1% larger than previously realized. The relative expanded uncertainty (k=2) of the NIST luminous flux scale is now 0.5%.

Keywords: Calibration, Integrating sphere, Lumen, Luminous flux, Photometer, Photometry, Radiant flux, Scale, Standards, Total Flux, Total luminous flux, Unit

---

Introduction

The NIST luminous flux scale was last realized in 1985 using a goniophotometer. The scale has since been maintained on a group of six primary standard lamps.[1] The luminous flux scale was based on the NIST spectral irradiance scale at that time, and was not tied to the present detector-based NIST illuminance scale[2,3] introduced in 1992. A new method for luminous flux scale realization using an integrating sphere has been studied at NIST theoretically.[4] An experimental realization predicted sufficient accuracy of this method for standard use.[5] This method (hereafter called "integrating sphere method") uses an integrating sphere with an opening to introduce a known amount of flux from an external source, which is compared to the luminous flux of an internal source to be calibrated.

Luminous flux scales are realized at many national laboratories using goniophotometers, which require a large dark room space and costly high precision positioning equipment. Care must be taken to reduce sources of errors such as stray light, shadowing by lamp holders, data acquisition intervals and timing, etc.[6-8] The integrating sphere method has the advantage that a conventional integrating sphere can be used with small modifications, and the sphere can still be used for ordinary substitution measurements. Measurements are accomplished faster, resulting in shorter operating time of lamps. In case the luminous intensity distributions of the internal lamps are not sufficiently uniform, it may be necessary to measure spatial distributions of the lamps with a goniophotometer to allow corrections for the spatial non-uniformity of the integrating sphere.

The integrating sphere method, with a slight modification of the design shown in previous work[4,5], has been applied to the NIST 2 m integrating sphere. Using this method, with more rigorous correction techniques, a new NIST luminous flux scale has been established based on the NIST illuminance scale. Corrections were made for the spatial non-uniformity and the incident angle dependence of the sphere response to reduce uncertainties in this method. A spectral correction was applied for the difference in color temperature of the external source and the internal source.

The theory, experimental procedures, results, uncertainty analysis, and the change of the magnitude of the NIST 1995 luminous flux unit are reported.

Theory and procedures of the integrating sphere method

Figure 1 shows the original geometry[4,5] of the integrating sphere design for this purpose. An opening is placed 135° away from the detector, and the flux from the external source is

introduced through a calibrated aperture placed in front of the opening. Baffle 2 is used to prevent the direct light of the internal source from passing out through the opening. The internal source can stay in the sphere when the flux from the external source is introduced into the sphere. The detector is exposed to the first reflection of the introduced flux from the external source in order to equalize the sphere responsivity for the internal source and that for the external source.

The luminous flux Φ_e (lm) from the external source introduced into the sphere is given by

$$\Phi_e = E_a \ S \tag{1}$$

where E_a is the average illuminance (lx) over the limiting aperture of known area S. Let k_a be the average illuminance factor, which is the ratio of the average illuminance to the illuminance E_c (lx) on the center of the aperture . Then Eq.(1) is rewritten as

$$\Phi_e = E_c \, k_a \ S \tag{2}$$

Once k_a is determined for the external source, only E_c needs to be measured as long as the alignment of the external source is reproduced in subsequent measurements. The sphere responsivity R_s is calibrated by measuring the external source,

$$R_s = y_e / \Phi_e \tag{3}$$

where y_e is the detector current for the external source. With the external source turned off and the internal source turned on, and if the integrating sphere were ideal, the total luminous flux Φ_i of the internal source would be obtained simply by

$$\Phi_i = y_i \ / \ R_s \tag{4}$$

where y_i is the detector current for the internal source. A self-absorption correction is not necessary if the internal source to be calibrated stays in the sphere when the external source is measured.

The response of the integrating sphere, however, is not uniform over the sphere wall, and corrections are necessary as has been previously reported.[4] The spatial response distribution function (SRDF), $K(\theta,\varphi)$ of the sphere, is defined as the sphere response for the same amount of flux incident on a point (θ,φ) of the sphere wall or on a baffle surface, relative to $K(0,0)$. $K(\theta,\varphi)$ can be obtained by measuring the detector signals while rotating a narrow beam inside the sphere. $K(\theta,\varphi)$ is further normalized by the sphere response to an isotropic point source. The normalized SRDF, $K^*(\theta,\varphi)$, is defined as

$$K^*(\theta,\varphi) = 4\pi K(\theta,\varphi) \Big/ \int_{\varphi=0}^{2\pi} \int_{\theta=0}^{\pi} K(\theta,\varphi)\sin\theta \, d\theta \, d\varphi \tag{5}$$

Using $K^*(\theta,\varphi)$, the spatial correction factor scf_e for the external source with respect to an isotropic point source is given by

$$scf_e = 1 / K^*(\theta_e,\varphi_e) \tag{6}$$

where (θ_e,φ_e) is the point on which the center of the illuminated area by the external source is located. It is assumed that the area illuminated by the external source is small enough so that $K^*(\theta_e,\varphi_e)$ represents the average SRDF over the area. The spatial correction factor scf_i for the internal source with respect to an isotropic point source is given by

$$scf_i = 1 \Big/ \int_{\varphi=0}^{2\pi} \int_{\theta=0}^{\pi} I^*_{rel}(\theta,\varphi) K^*(\theta,\varphi) \sin\theta \, d\theta \, d\varphi \tag{7}$$

where $I^*_{rel}(\theta,\varphi)$ is the normalized luminous intensity distribution of the internal source given by

$$I^*_{rel}(\theta,\varphi) = I_{rel}(\theta,\varphi) \Big/ \int_{\varphi=0}^{2\pi} \int_{\theta=0}^{\pi} I_{rel}(\theta,\varphi) \sin\theta \, d\theta \, d\varphi \tag{8}$$

where $I_{rel}(\theta,\varphi)$ is the relative luminous intensity distribution of the internal source. $I^*_{rel}(\theta,\varphi)$ is normalized so that its total luminous flux becomes 1 lm. Goniophotometry is necessary to measure $I_{rel}(\theta,\varphi)$, but corrections for scf_i (using goniophotometry data) may not be necessary if the internal sources have fairly uniform spatial distribution, with scf_i being very close to 1.

$K(\theta,\varphi)$ assumes normal incidence on the sphere wall. This applies for the internal source, but may not apply for the external source which is incident on the sphere wall at 45°. The SRDF for the external source with 45° incidence is defined as $K_{45}(\theta_e,\varphi_e)$, The incident angle dependence correction factor β is given by

$$\beta = K(\theta_e,\varphi_e) / K_{45}(\theta_e,\varphi_e) \tag{9}$$

If the spectral power distribution of the internal source is different from that of the external source, a spectral mismatch error occurs due to imperfect spectral responsivity matching of the sphere system (sphere + detector) to the spectral luminous efficiency function $V(\lambda)$. The spectral mismatch correction factor ccf_i^* of the internal source against Illuminant A (2856 K Planckian source) is given by

$$ccf_i^* = \frac{\int_\lambda S_A(\lambda) R_s(\lambda) \, d\lambda \int_\lambda S_i(\lambda) V(\lambda) \, d\lambda}{\int_\lambda S_A(\lambda) V(\lambda) \, d\lambda \int_\lambda S_i(\lambda) R_s(\lambda) \, d\lambda} \tag{10}$$

where $S_i(\lambda)$ is the relative spectral power distribution of the internal source, $S_A(\lambda)$ is that of the Illuminant A, and $R_s(\lambda)$ is the relative spectral responsivity of the sphere system. It should be noted that, even though the detector itself may be well matched to the $V(\lambda)$ function, the spectral responsivity curve of the sphere system may be shifted due to the spectral throughput of the integrating sphere. $R_s(\lambda)$ can be expressed as

$$R_s(\lambda) = R_d(\lambda)\, T_s(\lambda) \tag{11}$$

where $R_d(\lambda)$ is the relative spectral responsivity of the detector, and $T_s(\lambda)$ is the relative spectral throughput of the integrating sphere. The spectral transmittance of the diffuser should be included in either $R_d(\lambda)$ or $T_s(\lambda)$.

The spectral mismatch correction factor ccf_e^* of the external source against the Illuminant A is given by Eq.(10) with $S_i(\lambda)$ replaced by the relative spectral power distribution $S_e(\lambda)$ of the external source.

Taking these corrections into account, the sphere responsivity R_s' (for an internal source with uniform intensity distribution) is finally given by

$$R_s' = y_e\, ccf_e^*\, scf_e\, \beta\, /\, (\, E_c\, k_a\, S\,) \tag{12}$$

R_s' is determined with a particular internal source (a representative lamp) inside the sphere. If a different test lamp is measured, a self-absorption correction must be applied. The self-absorption correction factor α is obtained by

$$\alpha = y_{r,e} / y_{t,e} \tag{13}$$

where $y_{r,e}$ is the detector signal with the representative lamp inside the sphere, and $y_{t,e}$ is the detector signal with the test lamp inside the sphere, when only the external source is operated. Then the total luminous flux Φ_i (lm) of an internal source (test lamp) is obtained by

$$\Phi_i = y_i\ ccf_i^*\, scf_i\, \alpha\, /\, R_s' \tag{14}$$

Experimental Facility

Modified NIST 2 m integrating sphere

Figure 2 shows the geometry of the modified NIST 2 m integrating sphere used in this work. The sphere is coated with barium sulfate paint with a reflectance of 96 % to 98 % in the visible region. An opening of 10 cm in diameter was cut at a position 45° away from the detector.

The relative location of the detector and Baffle 1 was moved (rotated 90°) from the original design (**Figure 1**) to avoid installing the external source and other optics to hemisphere B which moves when the sphere is opened. The portion illuminated by the external source is located in the same geometry (135° from the detector). Baffle 1 (20 cm in diameter) is located at 50 cm from the sphere center. Baffle 2 (15 cm in diameter) is located at 60 cm from the sphere center. The effect of Baffle 2 is expected to be much smaller than reported in previous studies[4,5] because its size is much smaller relative to the size of the sphere. The detector views obliquely the entire portion of the sphere wall illuminated by the external source between the two baffles.

The detector is a $V(\lambda)$-corrected photometer of the same design as those used for the NIST illuminance scale[2)] with an opal diffuser (20 mm diameter) attached in front. It has a built-in transimpedance amplifier with gain settings from 10^4 to 10^{10} V/A calibrated at each range (except 10^{10} range) with an uncertainty† of 0.02 %. A built-in temperature sensor allows corrections for the photometer temperature drift. The linearity of the detector was measured to be constant over a flux range of 10^{-1} lm to 10^5 lm to within 0.05 % using a beam conjoiner system.[9] The detector is mounted so that the diffuser surface is flush with the sphere coating surface. The detector can be easily detached from the sphere for characterization.

A group of twelve 40 W (24 V, 1.7 A) opal-bulb incandescent lamps, operating at 2730 K with a base-up position, were used as "internal sources". These lamps, having ~500 lm, were calibrated to serve as the luminous flux primary standard lamps.

The power supply for the lamps and DVMs are computer controlled. The lamp current is stabilized on a feedback control to be within ±0.002 %. Each reading of the detector signal is sampled 20 times and averaged to reduce errors due to random fluctuations of the signal. The lamp current is measured with a current shunt calibrated with an uncertainty of 50 ppm.

External source set-up

Figure 3 shows the set-up for the external source consisting of a 1000 W frosted FEL type quartz halogen lamp operated at 2856 K. The lamp is mounted on a swing mount with an x-y translation stage. A He-Ne laser is used to define the optical axis for alignment. A mirror was affixed on the aperture plate to align the angle of the aperture to be perpendicular to the optical axis.

† Throughout this paper, uncertainty is given as relative expanded uncertainty with coverage factor k=2, thus a two standard deviation estimate.

The angular orientation of the lamp was aligned using an alignment jig (a mirror mounted on the bi-post base parallel to the center lines of the posts). The height and the lateral position of the lamp were aligned so that the filament center was on the optical axis. The path from the second screen (from the lamp) to the sphere opening was completely covered by a hood and the bottom plate. Black velvet was used for all the inner surfaces of the hood, the plate, the screens, and the aperture (except near the edges) to reduce stray light. Two stainless steel limiting apertures of 40 mm and 50 mm diameter, and 3 mm thick, are available for use. The area of the apertures was determined by the NIST Fabrication Technology Division by measuring the average diameter with an uncertainty of 5 μm, which corresponds to 0.03% in area (40 mm aperture). The aperture is placed as close to the opening as possible to minimize diffraction losses[10], which was calculated to be negligible (less than 0.01%).

The external lamp was placed at 70 cm from the limiting aperture to provide a sufficient flux level from the instrument (~2.7 lm with 40 mm aperture). The illuminance on the aperture plane was measured using a transfer photometer described in the *Calibration of the transfer photometer* section. The alignment of the transfer photometer was critical because of the fairly short distance to the source (70 cm). The transfer photometer has a holding plate which can be mounted interchangeably with the aperture. The position of the photometer on the holding plate was aligned, using an alignment telescope, so that the reference plane of the photometer and that of the limiting aperture coincide exactly when they were mounted. Once the photometer was aligned and fixed on the holding plate, the photometer and the aperture were exchanged easily reproducing the same position to within an uncertainty of 0.2 mm .

Calibration of the external source

NIST Illuminance Scale

Until recently, at NIST, the luminous intensity scale was based on the NIST spectral irradiance scale which was based on a gold point black body.[1] In 1992, a new luminous intensity (candela) scale was realized based on the absolute responsivity of detectors, either on absolute silicon detectors, or more recently on an absolute cryogenic radiometer.[2,3]

The photometric responsivities of the eight standard photometers are calibrated annually against the NIST spectral responsivity scale which is based on the cryogenic radiometer[11], thus providing the NIST illuminance scale. Luminous intensity (candela) is determined from the

illuminance measurement and geometrical considerations. The expanded uncertainty (k=2) of the illuminance scale realization is 0.39 %.[2] The standard photometers were calibrated in December 1994, and the luminous flux scale realization measurements were performed in February, 1995, to minimize errors due to the drift of the standard photometers with time.

Calibration of the transfer photometer

The illuminance from the external source on the aperture plane was measured using a transfer photometer. The transfer photometer is the same design as the NIST standard photometers[2] except that it has an opal diffuser (10 mm in diameter) in front. Since the transfer photometer measured illuminance of the FEL lamp at a fairly close distance (70 cm), a diffuser was added to reduce possible angular response errors. The photometer signal was corrected for the photometer temperature measured by the built-in temperature sensor.

The photometric responsivity of the transfer photometer was calibrated with the eight NIST standard photometers under illumination by the same frosted FEL lamp (operated at 2856 K) used as the external source, at a distance of approximately 3.5 m. The transfer measurement was performed before and after the flux scale realization measurements, and the average was taken. The responsivity of the transfer photometer reproduced within 0.07 %.

Illuminance distribution of the external source

The limiting apertures (40 mm and 50 mm in diameter) for the external source were placed at 70 cm from the external source, subtending an angle of ± 2° from the center of the source. Although the luminous intensity of the frosted FEL lamp was fairly uniform, the illuminance distribution of the FEL lamp at 70 cm distance was measured by spatially scanning the transfer photometer mentioned above to determine the average illuminance factor k_a in Eq.(2). The value of k_a was 0.9986 for the 50 mm aperture, and 0.9990 for the 40 mm aperture. The drift of the FEL lamp during this measurement was within 0.03 %.

Characterization of the integrating sphere

Spatial response distribution function (SRDF)

As described in the theory section, measurement of the SRDF is necessary to apply the correction for the spatial non-uniformity of the sphere response. The SRDF $K(\theta,\varphi)$ is the relative

sphere response for the same amount of flux incident on a point (θ,φ) of the sphere wall or on a baffle surface. $K(\theta,\varphi)$ was measured by rotating a beam source which was burning position insensitive. The source is made of a 6 V/1.2 W vacuum incandescent lamp equipped with a reflector (40 mm diameter) and a cylindrical hood (100 mm long). The inside of the hood is painted black, and the outside is painted white. The beam angle is ~10°. The burning position dependence of the lamp was tested using a closed tube (30 cm long). The lamp was fixed on one end of the tube and operated at a constant current. A $V(\lambda)$-corrected detector was placed on the other end of the tube. Neither the lamp voltage nor the detector output changed when the tube was rotated 360° around a horizontal axis. The SRDF measurements were made at 5° intervals for θ and 30° intervals for φ. Measurements were repeated three times. The last measurement was made with the φ angles shifted 15°. The scf_e values and scf_i values reproduced within 0.10 % and 0.03 %, respectively.

Figure 4 (a) and **(b)** shows the SRDF $K^*(\theta,\varphi)$ of the integrating sphere for the upper hemisphere and for the lower hemisphere, respectively. The polar coordinate (θ,φ) in the graphs is originated in the position of the detector as illustrated in **Figure 2**. φ=0 is the plane passing through the bottom of the sphere. The SRDF in the lower hemisphere is lower because of contamination. The luminous intensity distributions of the 40 W opal-bulb lamps, shown in **Figure 5**, were measured with the cooperation of PTB, Germany, using their goniophotometer. The polar coordinate of this data was converted (rotated 90°) to fit the coordinate of $K(\theta,\varphi)$ shown in **Figure 2**. The scf_e for the external source was calculated using Eq. (6) and determined to be 0.9870. The scf_i for the 40 W opal lamps was calculated using Eq.(7) and determined to be 1.0003, which turned out to be almost negligible.

The beam source rotating mechanism used in the SRDF measurement was not fully automated. The uncertainty of the ratio, scf_e/scf_i, is estimated to be 0.30 % from the drift of the beam lamp during measurement (within 0.20 %) and the uncertainty in the θ, φ angle setting (estimated to be 3°, which corresponds to 0.15% in sphere response at θ=135°, φ=90°) as well as a large scanning intervals of φ angle. This uncertainty value can be improved with better instrumentation.

Correction for the incident angle dependence of the sphere response

The SRDF is measured for normal incidence to the sphere wall. The light from the external source is incident at 45°. When the incident angle is different, the diffuse reflectance and the

BRDF (bidirectional reflectance distribution function) of the coating surface change,[12,13] which affect the sphere response. The spatial distribution of the first reflected light also changes. A test was performed to evaluate this effect as shown in **Figure 6**. The detector signals were compared when the beam source (used for the SRDF measurement) was placed in the center of the sphere and in the optical axis of the external source, irradiating the same part of the sphere wall. The difference in self-absorption at the two positions was measured using an auxiliary lamp, and found to be negligible. The incident angle dependence correction factor β given in Eq.(9) was determined to be 0.9966. The sphere response was 0.34 % higher at 45° than at 0° incidence, which was in approximate agreement with the data in reference[12]. The variation of the six readings of β was 0.06 % (two times the standard deviation of the mean).

Spectral mismatch correction

Since the color temperatures of the external source (2856 K) and the internal sources (2730 K) are different, spectral mismatch corrections were applied. The relative spectral power distributions of the sources were measured in one direction on the photometry bench using a spectroradiometer. The relative spectral responsivity $R_d(\lambda)$ of the detector (a diffuser is attached) was measured at the Spectral Comparator Facility[14] of NIST. The relative spectral throughput $T_s(\lambda)$ of the sphere was obtained by taking the ratios of the spectral irradiance on the detector port of the sphere in which a 500 W clear-bulb flux standard lamp was operated and the spectral irradiance of the same lamp measured on the photometry bench. The relative spectral responsivity $R_s(\lambda)$ of the total integrating sphere system was then obtained using Eq.(11). These spectral response curves are shown in **Figure 7.** All curves are normalized at 555 nm. Using Eq.(10), the spectral mismatch correction factors ccf_i^* and ccf_e^* were calculated to be 0.9982 and 1.0000, respectively. The uncertainty of the ratio, ccf_i^* / ccf_e^*, is estimated to be 0.04 % from the uncertainties of $T_s(\lambda)$ measurements (2 %), the detector spectral responsivity measurements (0.5 %), and the spectroradiometric measurements of the internal and the external sources (less than 30 K).

Luminous flux scale realization

Determination of the sphere responsivity

After the external source was stabilized for more than one hour, the illuminance E_c [lx] of

the external source and the detector currents y_e of the sphere detector with the 40 mm aperture and with the 50 mm aperture were measured alternately. E_c was measured not only with the transfer photometer, but also with three of the NIST standard photometers for cross check. Measurements were made in the following order: y_e(40 mm), y_e(50 mm), E_c(Transfer photometer), E_c(NIST photometer), y_e(40 mm). Measurement of each quantity was followed by a dark reading which occurred after covering the screen opening closest to the FEL lamp (**Figure 3**) with black velvet cloth. This entire set of measurements was repeated three times. The beginning and end values of y_e(40 mm) always reproduced to within 0.02 %. The sphere responsivity R_s' (A/lm; amperes/lumen) was calculated using Eq.(12). The variation of R_s' determined in the three runs was 0.04 % (two times the standard deviation of the mean). The R_s' values measured using the NIST standard photometers agreed with the results of the transfer photometer to within 0.09 %. There was always a 0.05 % disagreement between the results with the two different apertures, and the average was taken. This difference is considered to be due to a slight warp of the aperture plates which may have affected the effective distance to the FEL lamp. The 0.05 % difference in signal corresponds to 0.18 mm in distance, which was hard to recognize with the telescope.

Calibration of primary standard lamps

A group of twelve 40 W opal-bulb incandescent lamps were calibrated to serve as the total luminous flux primary standards. At the same time, eight 60 W inside frosted incandescent lamps were also calibrated to serve as working standards. The calibrations of these 20 lamps were performed twice, first, a day before the determination of the sphere responsivity, and second, the same day immediately after the determination of the sphere responsivity. The drift of the sphere responsivity during these calibrations (each lasted ~3 h) was checked by measuring a reference lamp at the beginning, the middle, and at the end of the calibration period. The reference lamp was known to reproduce its total luminous flux to within 0.02 % in the short term. The drift of the sphere responsivity during each calibration period was -0.12 %, which was caused probably by contamination of the sphere coating. The change of the sphere responsivity at the end of the first day and at the beginning of the second day was found to be negligible. The detector readings were all corrected for the drift of the sphere responsivity interpolated linearly. Self-absorption factors of all the 40 W and 60 W lamps, relative to the representative lamp, were measured using the external source. The total luminous flux values of all the lamps were then assigned according to Eq.(14). The scf_i values for the 60 W working standard lamps were assumed to be unity since these lamps

have similar luminous intensity distributions. When the assigned luminous flux values of each lamp in two runs were compared, all the lamps reproduced to within ± 0.06 %.

Uncertainty budget

The uncertainty budget of the luminous flux scale realization is shown in Table 1. The uncertainty value of each factor is explained in the previous sections. The overall uncertainty of the luminous flux scale realized on the 40 W opal-bulb lamps is estimated to be 0.53 % (relative expanded uncertainty, k=2).

Comparison with a goniophotometer

In order to further verify the uncertainty of this integrating sphere method, the total luminous flux values of two of the 40 W opal-bulb lamps mentioned above were compared with values measured by a goniophotometer in PTB, Germany. The goniophotometer was calibrated against the NIST illuminance scale so that only the difference in the spatial integration method was compared without influence of the difference in illuminance scale. This measurement was conducted in November 1993, and the lumen values of these two lamps were transferred to four other 40 W opal-bulb lamps when returned to NIST. The average difference, $(\Phi_s-\Phi_g)/\Phi_g$, of the the luminous flux of these 6 lamps Φ_s measured by the sphere and Φ_g by the goniophotometer was 0.20 % ± 0.17 % (two times the standard deviation of the mean).

Change of the NIST luminous flux unit

In the 1985 CCPR international intercomparison, the magnitude of the NIST (NBS at that time) luminous flux unit was 1.0 % smaller than the world mean.[15] The scale used at that time, and serving as the luminous flux scale until now, was maintained on six primary standard lamps. The twelve 40 W opal-bulb lamps calibrated here were compared with these six previous primary standard lamps. The result shows that the magnitude of the NIST 1995 luminous flux unit is 1.1 % larger than the previous unit. In other words, the luminous flux values measured on the new scale are 1.1 % lower than the values measured on the previous scale. The difference of the magnitude of the luminous flux units between NIST and PTB, (PTB-NIST)/NIST, is now reduced to 0.4 % from 1.5 % in 1993[16].

Conclusion

The NIST 1995 luminous flux scale has been established using a new integrating sphere method. The calibration of 12 standard lamps is accomplished for use in routine substitution photometric methods. The total luminous flux measured using the integrating sphere method agreed with the values obtained from a goniophotometer to within 0.2 %. The magnitude of the new NIST luminous flux unit is 1.1% larger than the previous unit, and hence, lumen values measured with the new scale will be 1.1 % smaller than previously reported. The relative expanded uncertainty (k=2) of the new scale is 0.53 %. The new NIST luminous flux scale will be disseminated to the NIST photometric calibration services beginning January 1996.

While the correction factor scf_e for the external source is significant, the correction factor scf_i for the internal sources is insignificant. Goniophotometry is not essential in this method if the internal lamp has fairly uniform luminous intensity distributions. It should be noted, however, that the spatial correction factors will be larger with lower reflectance of the sphere coating. Variation of scf_i for various types of lamps under different sphere reflectances should be investigated.

Major uncertainty factors in the realized scale (except for the uncertainty of the illuminance scale) are those of the spatial correction factor scf_e and alignment of the transfer photometer and the apertures. The overall uncertainty will be reduced by improving the accuracy of SRDF measurements and the alignment technique.

The spatial correction technique using the SRDF is also useful for conventional substitution measurements. Using this technique, directional sources such as reflector type lamps and LEDs can be measured more accurately in an integrating sphere. Only rough data on the relative luminous intensity distribution is required.

The integrating sphere method will also be useful in the total spectral radiant flux scale realization, which is rather difficult with a goniophotometer. Investigation of this application is underway at NIST.

Acknowledgement

The author expresses sincere thanks to Dr. G. Sauter of PTB, Germany for his kind support in the measurements using PTB goniophotometer and for fruitful discussions.

References

1. Booker, R. L. and McSparron, D. A. 1987. *Photometric Calibrations,* NBS Special Publication 250-15
2. Cromer, C. L., Eppeldauer, G., Hardis, J. E., Larason, T. C. and Parr, A. C.; 1993. National Institute of Standards and Technology detector-based photometric scale," *Applied Optics* **32**-16, 2936-2948
3. Ohno, Y. 1994. The detector-based candela scale and related photometric calibration procedures at NIST. *J.IES* **23**-1 : 89-97.
4. Ohno, Y. 1994. Integrating sphere simulation: Application to total flux scale realization. *Applied Optics* **33**-13: 2637-2647.
5. Ohno, Y. 1995. New Method for Realizing a Total Luminous Flux Scale using an Integrating Sphere with an External Source, *J. IES* **24**-1: 106-115
6. CIE Publication No.84. 1987. Measurements of Luminous Flux
7. Bastie, J.; Andasse, B.; Foucart, R. 1991. Luminous flux measurements with a goniophotometer; study of time effects on data collection. *CIE Proceedings 22nd Session*, 1-1, Division 2 :45-47
8. Hu, R.S. 1991. Importance of axis alignment in goniophotometry. *CIE Proceedings 22nd Session*, 1-1, Division 2: 21-22
9. Thompson, A. and Chen, H. 1994, Beamcon III, a Linearity Measurement Instrument for Optical Detectors, *J. Res. NIST* **99**-6: 751-755
10. Blevin, W. R. 1970, Diffraction losses in radiometry and photometry, *Metrologia* **7**: 39-44
11. Houston, J. M., Cromer, C. L., Hardis, J. E., and Larason, T. C. 1993. Comparison of the NIST High-Accuracy Cryogenic Radiometer and the NIST Scale of Detector Spectral Response, *Metrologia* **30**-4: 285-290
12. Venable, W. H., Hsia, J. J., and Weidner, V. R. 1977. Establishing a Scale of Directional-Hemispherical Reflectance Factor I: The Van den Akker Method, *J. R. NBS*, **82**-1: 29-55
13. CIE Publication No.46. 1979. A Review of Publications on Properties and Reflection Values of Material Reflection Standards
14. Zalewski, E. F. 1988. NBS Measurement Services: The NBS Photodetector Spectral Response Calibration Transfer Program, *National Bureau of Standards, Special Publication 250-17*.
15. CCPR Rapport de la 11e session 1986, BIPM, Pavillon de Breteuil, F-92312, Sèvres Cedex, France
16. Ohno, Y. and Sauter, G. 1995, 1993 Intercomparison of photometric units between NIST and PTB, *J. Res. NIST*, **100**-3: 227-239

Figure captions

Figure 1 – Basic geometry of the integrating sphere.

Figure 2 – Geometry of the modified NIST 2 m integrating sphere.

Figure 3 – Set-up for the external source.

Figure 4 – SRDF of the integrating sphere. (θ=0 is at the detector. φ=0 is the plane passing through the bottom of the sphere.)
(a) Upper hemisphere, (b) Lower hemisphere

Figure 5 – Luminous intensity distribution of a 40 W opal-bulb lamp.

Figure 6 – Measurement of the incident angle dependence.

Figure 7 – Spectral responsivity of the integrating sphere system.

Table 1. Uncertainty budget for the NIST 1995 luminous flux scale

Factor	Relative expanded uncertainty, k=2 [%]	
Uncertainty of the determination of Φ_e		0.41
The NIST Illuminance scale realization[2]	0.39	
Ave. longterm drift of the standard photometers (2 months)	0.03	
Transfer to the transfer photometer	0.07	
Transfer photometer position alignment (±0.2 mm)	0.06	
Aperture alignment (difference of the two apertures)	0.05	
Aperture area	0.03	
Average illuminance factor k_a	0.03	
Drift of the external source during calibration	0.02	
Uncertainty of the lamp luminous flux with respect to Φ_e		0.32
Spatial correction factor scf_i / scf_e	0.30	
Incident angle dependence correction factor β	0.06	
Spectral mismatch correction factor ccf_i^* / ccf_e^*	0.03	
Self-absorption correction factor α	0.03	
Random variation in the R_s determination	0.04	
Detector linearity	0.05	
Reproducibility of the standard lamps	0.06	
Overall uncertainty of the NIST 1995 luminous flux scale		0.53

Discussion

Dr. Ohno provides a clear and complete description of the method of realization of the luminous flux scale at NIST. This new method represents a major accomplishment due to the improved accuracy of the luminous flux standards. My concerns are perhaps peripheral to the content of the paper but basic to the use of the results being explained in the paper.

First, the benefit of reduced operating time on a lamp during calibration seems to be based on the assumption that the luminous intensity distribution of the lamp to be calibrated is sufficiently uniform. This implies that this method will be used for a limited number of lamp types which meet some criteria of uniformity of intensity distribution. Is this method directly applicable to producing standards of luminous flux from four foot linear lamps? Since your conclusions indicate that the method can be applied to reflector lamps to create standards of total forward lumens when "Rough" data on intensity distribution is available, is there a limiting distribution variation which would require goniophotometric evaluation? What is the impact of the sphere diameter on the range of applicability of this method with respect to the intensity distribution limitations and the physical dimensions of the lamp? Does one still retain the benefits of reduced time to create the standards and reduced operating time on the lamps? Does NIST have the goniophotometric capability of developing standards from lamps with non-uniform intensity distributions?

The concerns which Dr. Ohno addresses in his experimental approach apply as well to the derivation of secondary standards from the primary luminous flux distribution standards. These include changes in intensity distribution of the source, the spatial correction factors and the spectral correction factors. It would be very useful if the author would address these and other issues involved in the transfer of the newly realized luminous flux scale to secondary and working standards of various types. This seems particularly important as Dr. Ohno's work relies heavily upon modeling of the sphere to predict location of baffles, sources and the effects of non-uniform sphere reflectance. These calculations would seem necessary in evaluating the ability to transfer the calibration to secondary and working standards. Representative results of such calculations or the methods of performing such calculations would be of value in the next step of a secondary laboratory's maintenance of the lumen.

Dr. Ronald O. Daubach
OSRAM SYLANIA INC.

Dr. Ohno presents an interesting and comprehensive description of a new photometric calibration scheme developed at NIST. Characterization of the spatial response distribution function is, in my opinion, the most critical element of this scheme. The spatial response function of the surface area illuminated by the external source must be carefully characterized. I assume that this particular area was characterized since a correction for incident angle was determined at this location. You state that the sphere responsivity drift over each calibration period was -0.12 % (which was probably caused by contamination of the sphere coating). Was there any drift in the spatial response distribution function over that same time period? Was there any attempt to

characterize a drift in the spatial response distribution function over time?

In your paper you state that the externally illuminated surface area is small enough to assume an uniform spatial response function over that area. In your conclusion, you state that directional sources such as reflector type lamps can be measured with this approach. However, with a flood beam pattern you cannot assume that the spatial response function is uniform over the first illuminated area. How do you address this matter?

David Ellis
Inchcape Testing Services
ETL Testing Laboratories

Thank you Dr. Ohno for a very comprehensive and interesting presentation on the realization of the new NIST luminous flux scale. Your analytical work behind the flux realization is very thorough and complete.

You state that your new scale is 1.1 % higher than your existing scale and the comparison of goniophotometric measurements to the sphere measurements are within 0.2 %. Was the PTB Germany goniophotometer calibrated using the new or the old NIST scale? If the 1985 scale was based on goniophotometer readings and the new goniophotometer readings relate closely to the sphere readings, why was the 1985 flux scale inaccurate? Is this change in the flux scale a result of using the detector-based illuminance scale of 1992?

Your work on factoring for the spatial non-uniformities of the integrating sphere measurements is very detailed. Do you feel that this method should be applied when using an integrating sphere for measurements of reflector type lamps? Will you be continuing this work and possibly be preparing a practitioner's guide?

Again, I would like to commend Dr. Ohno for his work on the new flux scale and was very happy to see the closer alignment between the NIST scale and those of the other standards organizations.

Ronald Gibbons
Philips Lighting

Author's response

To Dr. R. Daubach

The points Dr. Daubach raised are important in applying the integrating sphere method for a variety of test lamps. Only two types of lamps were used in this work, and only one type of them was characterized goniophotometrically. Whether the intensity distribution of test lamps should be measured or not depends on what integrating sphere is used and what level of accuracy is desired. To establish a criteria, more data on different types of lamps under different conditions should be accumulated.

However, there is a benefit of reduced operating time in the integrating sphere method for the following reasons: (1) I expect that the spatial nonuniformity errors for flux standard lamps and A-line type lamps are probably negligible if the sphere is similar to the one at NIST, (2) If the intensity distribution data is available from manufacturers or testing laboratories, such data will probably suffice, (3) If data is not available, one representative lamp can be measured and the data

can be used for other lamps of the same type, and (4) when the lamps are recalibrated, the previous intensity distribution data can be used repeatedly.

In principle, the integrating sphere method, is applicable to any type of lamps. There will be no problem for 4-foot fluorescent lamps as long as the lamp and the holder do not intercept the flux from the external source. The intensity distribution can be calculated as a line source. Reflector lamps can be treated the same way as other lamps, with the spatial correction being essential. However, at the moment, the integrating sphere method at NIST is only used to calibrate the primary working standard incandescent lamps. All the test lamps are measured by substitution with the working standard lamps.

The size of the sphere is certainly another important issue. When the sphere is too small relative to the lamp size, there would be errors due to the nonuniformity of the sphere response for the position of the source element. Also, a large self-absorption of the lamp would affect SRDF and *ccf*. The initial illuminance on the sphere wall would deviate from what is calculated from far-field goniophotometric data. However, I believe that the decisive factor for the sphere size is the volume of the sphere required to keep the ambient temperature of the lamp stable.

I would like to make it clear that, both in case of scale realization and transfer measurement, the modeling of the sphere is not an essential factor for accuracy. Modeling was only used to predict the performance of the designed spheres. The accuracy depends on the actual correction measurements. This is also the case with transfer measurements. For best possible accuracy, corrections must be and can be made for spatial nonuniformity, spectral mismatch, self-absorption, and the size (length) of the source. The self-absorption of discharge lamps should be studied because it is reported to change when the lamps are turned on.

Lastly, a goniophotometer is necessary to study some of the issues discussed here. We plan to install a new, small goniophotometer at NIST for experimental purposes.

To D. Ellis

As Mr. Ellis pointed out, the correction for the spatial nonuniformity of the sphere response for the external source is the most critical element of this method. The gradient of the SRDF function around the hot spot was measured along the θ and φ directions to determine the uncertainty resulting from the angle alignment errors of the rotating beam source. When the incident angle effect was measured, the laser beam (used for alignment of the external source setup) was used to align the beam source. Another point to note is that the coating of the NIST sphere was not in the best conditions. If a newly coated sphere is used, the SRDF should be more smooth and the measurement will be less critical.

The sphere responsivity is determined by $\rho/(1-\rho)$ and thus very sensitive to the sphere coating condition. The sphere responsivity drift of 0.12 % should not have affected the SRDF which is mostly determined by the surface reflectance and the geometric factor. Our measurement data also imply no change of the SRDF after the lamp calibration. I expect that the SRDF is stable for a long time, but we do not rely on its longterm stability. The SRDF will be measured every time the scale is realized, and its stability will be evaluated. If the integrating sphere method is to be used for daily calibration of test lamps, the longterm stability of the SRDF should be taken into account as Mr. Ellis pointed out.

In my paper, I suggested that reflector type lamps can be measured more accurately by

applying the spatial correction technique *in the substitution method*. No test lamps are measured in place of the external source in the scale realization setup. The flood beam pattern of reflector lamps should be taken into account by using Eq.(7) especially when the beam angle is large.

To R. Gibbons

When the comparison measurement was made at PTB, the goniophotometer was calibrated against the NIST 1992 candela scale which was almost the same as the current NIST candela scale of 1995. Therefore, as you presumed, the 1.1 % difference resulted partly from the change of the NIST candela scale which occurred in 1992 (~0.6 %, half of which resulted from the change of the international temperature scale in 1990).

Regarding your questions on reflector type lamps, we already have calibration services available at NIST for luminous flux of reflector type lamps. We apply the spatial correction technique based on the intensity distribution data submitted by the customer.

The IES Testing Procedure Committee, which I am a member of, has established a project with a goal of publishing a guide for total luminous flux measurement. There are still many peripheral issues to clarify and I would like to continue working in this area to contribute to the guide.

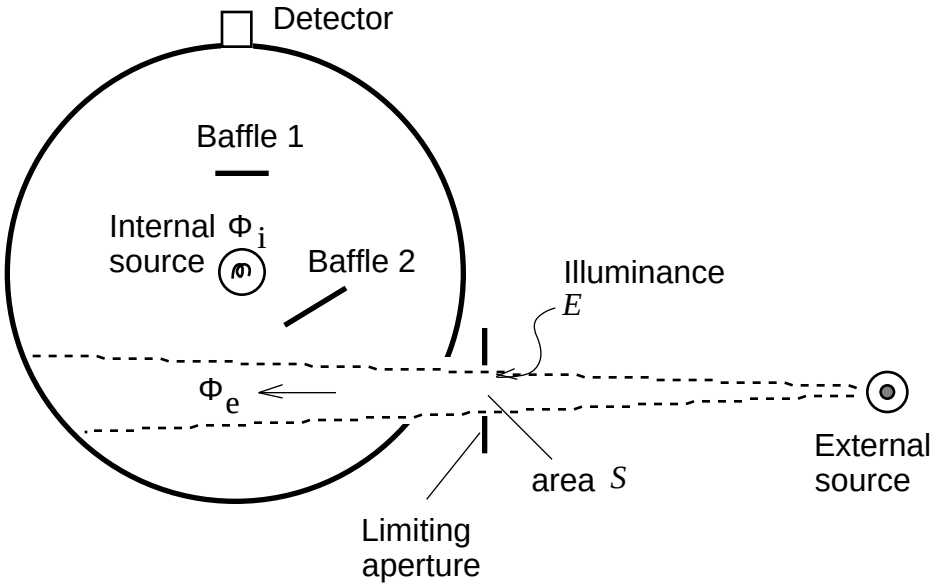

Figure 1 - Basic geometry of the integrating sphere

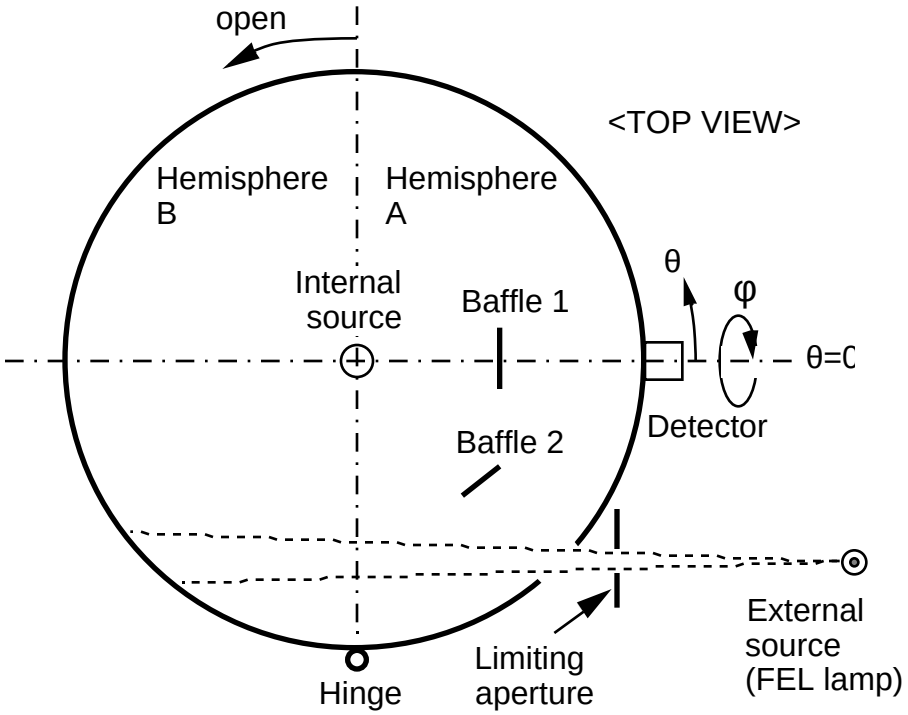

Figure 2 – Geometry of the modified NIST 2-m integrating sphere.

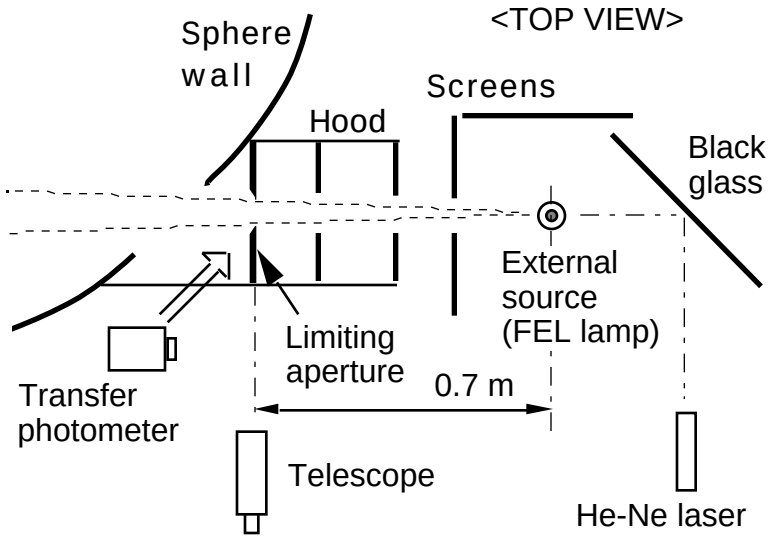

Figure 3 – Set-up for the external source

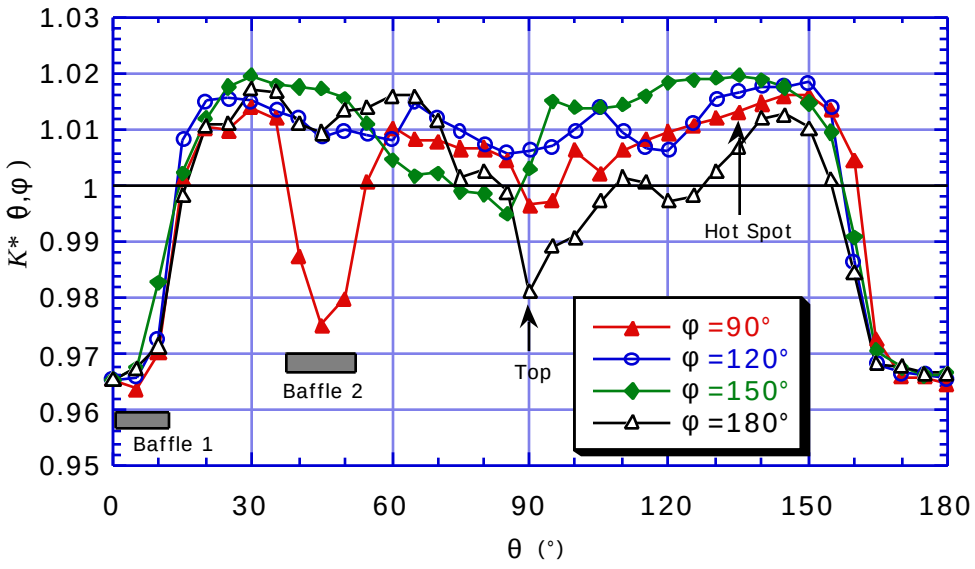

(a) Upper hemisphere

Figure 4 – SRDF of the integrating sphere. (θ=0 is at the detector. φ=0 is the plane passing the bottom of the sphere.)

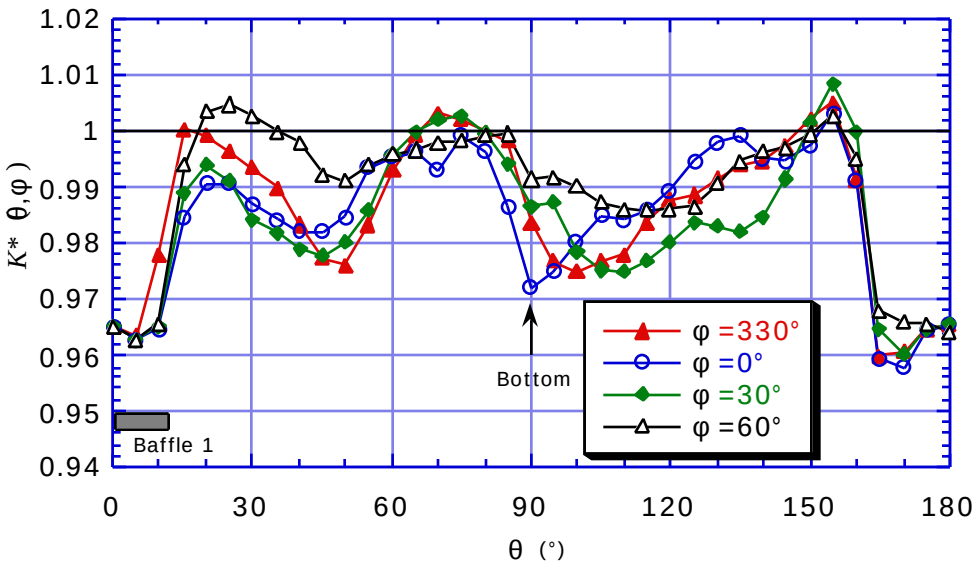

(b) Lower hemisphere

Figure 4 – SRDF of the integrating sphere. (θ=0 is at the detector. φ=0 is the plane passing the bottom of the sphere.)

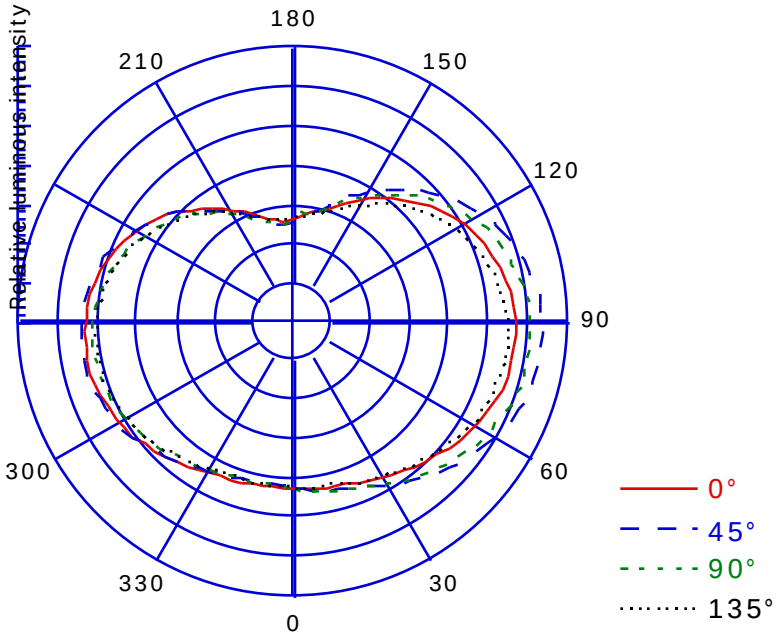

Figure 5 – Luminous intensity distribution of a 40W opal bulb lamp.

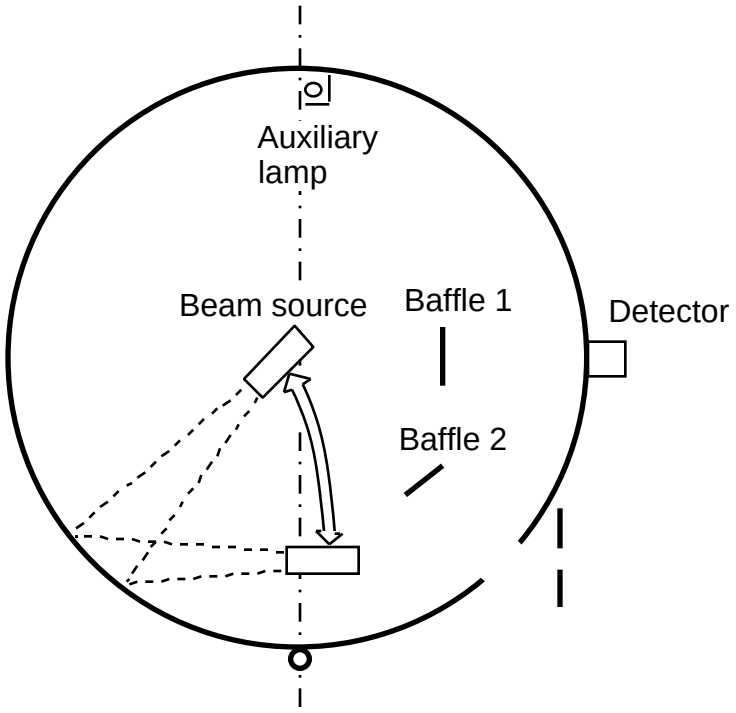

Figure 6 – Measurement of the incident angle dependence

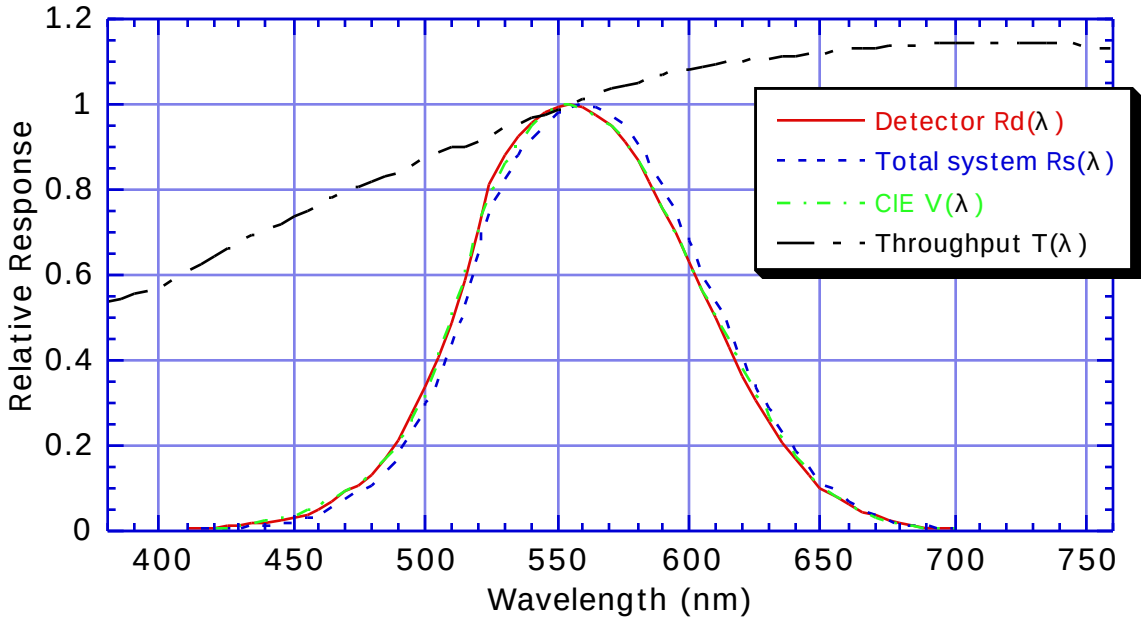

Figure 7 – Spectral responsivity of the integrating sphere system